Chemical Science

ROYAL SOCIETY OF CHEMISTRY

EDGE ARTICLE

View Article Online
View Journal | View Issue

Cite this: *Chem. Sci.*, 2021, **12**, 5898

All publication charges for this article have been paid for by the Royal Society of Chemistry

One tool to bring them all: Au-catalyzed synthesis of B,O- and B,N-doped PAHs from boronic and borinic acids†

Omar Ouadoudi,‡ Tanja Kaehler,‡ Michael Bolte, Hans-Wolfram Lerner and Matthias Wagner *

Received 28th January 2021
Accepted 16th March 2021

DOI: 10.1039/d1sc00543j

rsc.li/chemical-science

The isoelectronic replacement of C=C bonds with $^{-}$B=N^{+} bonds in polycyclic aromatic hydrocarbons (PAHs) is a widely used tool to prepare novel optoelectronic materials. Far less well explored are corresponding B,O-doped PAHs, although they have a similarly high application potential. We herein report on the modular synthesis of B,N- and B,O-doped PAHs through the [Au(PPh$_3$)NTf$_2$]-catalyzed 6-*endo*-dig cyclization of BN–H and BO–H bonds across suitably positioned C≡C bonds in the key step. Readily available, easy-to-handle *o*-alkynylaryl boronic and borinic acids serve as starting materials, which are either cyclized directly or first converted into the corresponding aminoboranes and then cyclized. The reaction even tolerates bulky mesityl substituents on boron, which later kinetically protect the formed B,N/O-PAHs from hydrolysis or oxidation. Our approach is also applicable for the synthesis of rare doubly B,N/O-doped PAHs. Specifically, we prepared 1,2-B,E-naphthalenes and -anthracenes, 1,5-B$_2$-2,6-E$_2$-anthracenes (E = N, O) as well as B,O$_2$-containing and unprecedented B,N,O-containing phenalenyls. Selected examples of these compounds have been structurally characterized by X-ray crystallography; their optoelectronic properties have been studied by cyclic voltammetry, electron spectroscopy, and quantum-chemical calculations. Using a new unsubstituted (B,O)$_2$-perylene as the substrate for late-stage functionalization, we finally show that the introduction of two pinacolatoboryl (Bpin) substituents is possible in high yield and with perfect regioselectivity *via* an Ir-catalyzed C–H borylation approach.

Introduction

The targeted doping of polycyclic aromatic hydrocarbons (PAHs) with p-block atoms is a powerful tool to create new molecules for applications as diverse as drug development, materials science, and catalysis.[1] Especially the isoelectronic replacement of a non-polar C=C bond with a polar $^{-}$B=N^{+} bond can substantially influence the π-electron distribution and frontier-orbital energies of the resulting B,N-PAH and thus lead to chemical and physical properties that differ considerably from those of the corresponding carbonaceous congener ("BN/CC isosterism").[2] By varying the positions,[3] orientations, and number of $^{-}$B=N^{+} units within the molecular framework, a greatly expanded structural and chemical space becomes accessible.[4–15] In addition, breaking the symmetry of a molecular scaffold through the introduction of a $^{-}$B=N^{+} unit often allows late-stage functionalizations with higher regioselectivities than in the case of the parent PAH.[16] Because of these appealing features, considerable research efforts are currently being made to develop novel B,N-PAHs. Although many synthesis approaches are still based on individual solutions of limited scope, the following more general strategies have already emerged. (i) *B–N/B–C-bond formation cascades*: the B–N bond is formed first, followed by an intramolecular electrophilic borylation reaction with a suitably positioned aryl, vinyl, or alkynyl group (Scheme 1a).[17–21] (ii) *C–C-bond formation/oxidation cascades*: a ring-closing metathesis (RCM) is conducted on an already established B–N moiety and a subsequent oxidation step generates the conjugated π system (Scheme 1b).[22,23] (iii) *Photochemical or exciton-driven C=B-bond formation*: starting from B–N adducts with N-heteroaryl-benzyl backbones, the elimination of HR′ (R′ = alkyl, aryl), which occurs either upon UV/vis irradiation or upon application of an electric current to a corresponding electroluminescent device, closes the conjugation pathway (Scheme 1c).[24,25]

Compared to B,N-PAHs, analogous B,O-PAHs have been largely neglected, although a first derivative, 10-hydroxy-9,10-oxaboraphenanthrene, was published by Dewar *et al.* as early

Institut für Anorganische und Analytische Chemie, Goethe-Universität Frankfurt, Max-von-Laue-Straße 7, D-60438 Frankfurt (Main), Germany. E-mail: matthias.wagner@chemie.uni-frankfurt.de;

† Electronic supplementary information (ESI) available. CCDC 2058862–2058872, 2068160, and 2068161. For ESI and crystallographic data in CIF or other electronic format see DOI: 10.1039/d1sc00543j

‡ Contributed equally.

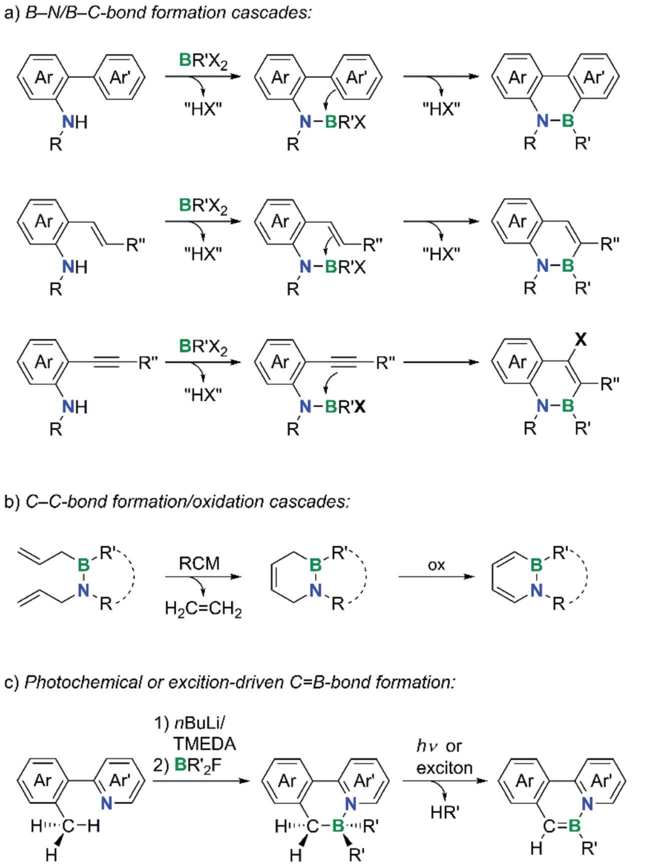

Scheme 1 Common strategies for the synthesis of B,N-doped PAHs. (RCM = ring-closing metathesis).

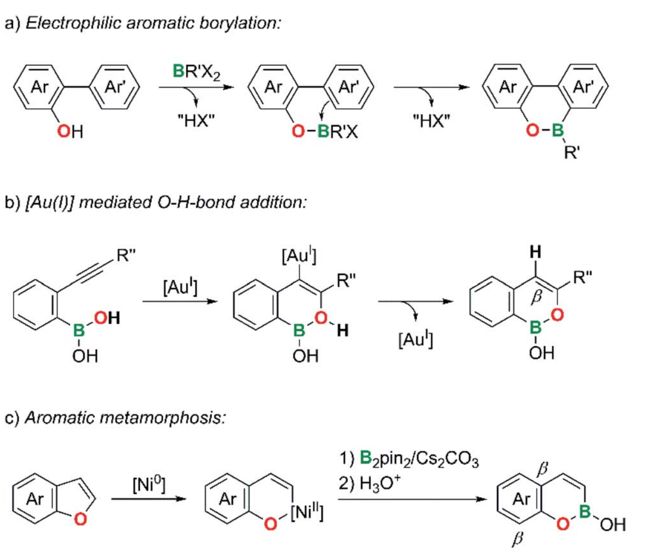

Scheme 2 Common strategies for the synthesis of B,O-doped PAHs.

as in 1960.[26] Still today, the majority of known B,O-PAHs contains the structural motif of a 9,10-oxaboraphenanthrene,[27–42] likely due to its convenient accessibility *via* B–O-bond formation/electrophilic aromatic borylation sequences (Scheme 2a; compare the analogous B,N case shown in Scheme 1a).[26–33]

A second class of B,O-PAHs with a reasonably large number of members are 1,2-B,O-naphthalenes. Sheppard *et al.* and Gong *et al.* selected *o*-alkynylphenyl boronic acids as the starting materials and used the Au- or Pd-catalyzed intramolecular addition of a BO–H bond to the C≡C bond in the final cyclization step (Scheme 2b).[43–46] Yorimitsu *et al.* prepared an isomeric 2,1-B,O-naphthalene through Ni- or Mn-catalyzed O–C-bond activation of benzofurans and subsequent insertion of a [Bpin]$^-$ fragment generated by heterolysis of bis(pinacolato) diboron, pinB–Bpin ("aromatic metamorphosis"; Scheme 2c).[47,48]

Even the limited information available on the chemical properties of B,O-PAHs reveal some distinct patterns: (i) due to the higher electronegativity and weaker π-donor ability of O relative to the N atom, B,O-PAHs tend to be less aromatic and more Lewis acidic than corresponding B,N-PAHs.[28,34,49–55] (ii) The 1,2-B,O-naphthalenes shown in Scheme 2b possess a relatively low stability due to the electron-rich C atom at the position β to the O atom ("boron enolates").[43–45] The associated peculiar reactivities of certain B,O-PAHs make them valuable synthetic intermediates for aldol reactions, aminations, Suzuki–Miyaura C–C couplings, Chan–Lam C–O couplings, and the formation of lactones by deborylative CO insertion.[29,35–37,43,44,47,56]

On the other hand, if the β position is embedded into an aromatic benzene ring (as in the cases of the isomeric 2,1-B,O-naphthalenes shown in Scheme 2c) and the B atom is equipped with an appropriate substituent,[57] the resulting B,O-PAHs can become sufficiently inert to serve as luminescent materials for optoelectronic applications.[31–33,38,39,41] It is also important to note in this context that the steric demand of an O atom is even lower than that of a CH or NH fragment in analogous B- or B,N-PAHs. This promotes a coplanar conformation between the respective B,O-heterocycle and, *e.g.*, B-bonded phenyl substituents and can thus contribute to the increase of conjugation lengths and the extension of the frontier orbitals from the oxaborin moiety to the phenyl ring.[38,47,52,58–60]

If one proceeds further from B,E-PAHs to $(B,E)_n$-PAHs with E = N or O and $n > 1$, the available information again becomes dramatically less,[9,11,13,30,32,39,54,55,61–78] which is unfortunate, because some evidence has already been gathered that the number n of embedded $^-$B=E$^+$ units significantly influences the chemical and physical properties of corresponding compounds.[30,54,68,72,79] Thus, new atom-economic strategies for the construction of $(B,E)_n$-PAHs, which ideally avoid the use of sensitive boron halides, sophisticated organometallic reagents, or forcing reaction conditions, are still in demand. The most time and cost-efficient approach would have to be sufficiently modular to implement both E = N and O *via* closely related reaction protocols. Some of these conditions are met by recently discovered ring-expansion reactions on five-membered ring precursors, which result in the insertion of one E atom into an endocyclic B–C bond. This way, boroles or 9-borafluorenes have been converted to 2,1-B,N/2,1-B,O-benzenes or 10,9-B,N/10,9-B,O-phenanthrenes, respectively.[41,53,54,80–85]

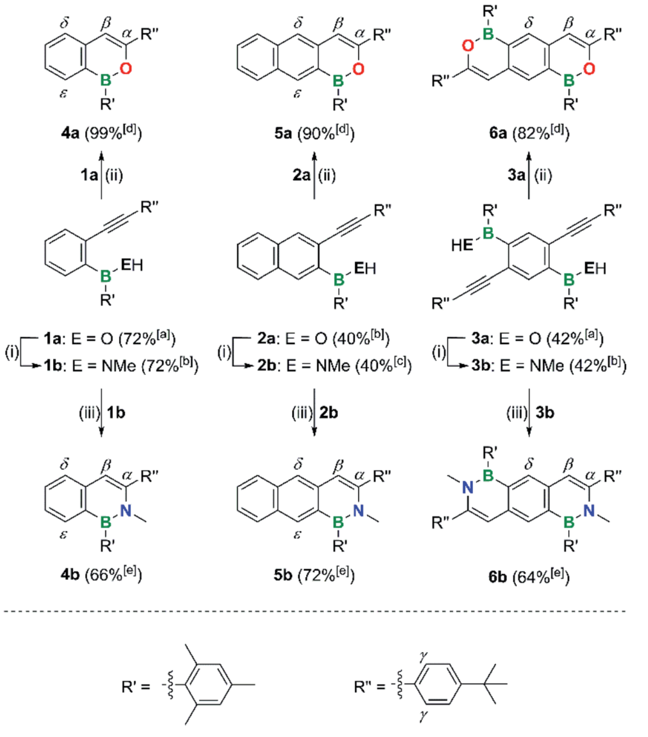

Scheme 3 Synthesis of compounds **4a,b–6a,b**. Reagents and conditions: (i) 1–2 equiv. $(Me_3Si)_2NMe$, C_6D_6, 120 °C, 2–3 d, sealed NMR tube. (ii) 1–2 mol% $[Au(PPh_3)NTf_2]$, $CHCl_3$, room temperature, 10 min. (iii) 5 mol% $[Au(PPh_3)NTf_2]$, $CDCl_3$, 60 °C, 4–48 h. [a] Overall yield over two steps from commercially available chemicals. [b] Overall yield over three steps from commercially available chemicals. [c] Overall yield over four steps from commercially available chemicals. [d] Yield of the final cyclization step. [e] Yield of the final cyclization step without isolation of **1b–3b**.

Inspired by the well-established oxypalladation of alkynes and Sheppard's above-mentioned work,[43] our group herein discloses a straightforward protocol for the synthesis of $(B,N)_n$- and $(B,O)_n$-PAHs. The main structural motif present in all synthetic intermediates employed is that of an *o*-alkynyl-substituted aryl boronic or borinic acid (Scheme 3). These intermediates can either be cyclized directly with the help of a $[Au^I]$ catalyst or first transformed into the corresponding aminoboranes and then cyclized using the same $[Au^I]$ catalyst. Our approach offers the following advantages: (i) the chemistry of boronic and borinic acids is nowadays very well explored and most derivatives can easily be handled, purified, and stored.[86] (ii) The possibility to decide in the last step before cyclization whether a B,N- or B,O-PAH should be prepared guarantees maximum efficiency. (iii) The protocol is applicable to the synthesis of both single and multiple B,E-doped PAHs. Our approach differs from all other strategies in that the cyclization step relies on the formation of C–N/O bonds.

As a proof-of-principle, we have already produced $(B,N)_2$- and $(B,O)_2$-perylenes *via* our method.[55] In our present work, we extend the scope of the reaction to (double) B,N/O-doped naphthalenes and anthracenes. It will also be shown that OBO- and NBO-doped phenalenyls are becoming accessible, the latter having no precedent in the literature.

Results and discussion

Syntheses

The *o*-alkynyl-substituted aryl borinic and boronic acid precursors **1a–3a** and **7a** required for the preparation of the $(B,O)_n$- and $(B,N)_n$-PAHs **4a,b–6a,b** and **8a–c** (Schemes 3 and 4) were synthesized starting from readily accessible mixed bromo(iodo)arenes. Negishi-coupling protocols were employed for the selective introduction of the alkynyl substituents at the iodinated C atoms. The subsequent borylation reactions were performed by Br/Li exchange with *t*BuLi, quenching of the resulting aryl lithium intermediates with $MesB(OMe)_2$ or $B(OMe)_3$, and aqueous acidic workup (see the ESI† for full details). The electronegative F_3C group in **7a,b** and **8a–c** is a remnant of the synthesis of 2-bromo-1,3-diiodo-5-(trifluoromethyl)benzene from 1-bromo-4-(trifluoromethyl)benzene and served to direct the two I atoms to the *ortho* positions of the Br substituent during electrophilic aromatic iodination. F_3C also proved to be a useful ^{19}F NMR-spectroscopic handle. The $tBuC_6H_4$ moieties were chosen with the aim to increase the solubilities of the obtained intermediates and products in organic solvents. Moreover, these substituents offer some steric shielding to the otherwise fully exposed reactive β-CH sites (see above). Finally, the intense *t*Bu signals in the sparsely populated alkyl regions of the ^1H NMR spectra of **1a,b–8a–c** effectively reveal the presence of possible side products and are thus a good measure of the selectivities of the desired conversions.

The B,O precursors **1a–3a** were cyclized using the catalyst $[Au(PPh_3)NTf_2]$ in $CHCl_3$.[43,55] Regardless of the presence of the bulky Mes substituents, which serve to protect the B atoms during workup, the reactions took place already at room temperature, required no more than a few minutes for completion, and gave yields in the range 82–99% (Scheme 3; all cyclizations were quantitative according to NMR).

The mono- or ditopic borinic acids **1a–3a** were transformed into the corresponding (methylamino)boranes by heating with $(Me_3Si)_2NMe$ in C_6D_6 (1–2 equiv., 120 °C, 2–3 d, sealed NMR tube). After the quantitative conversion was confirmed by NMR spectroscopy, the solvent was changed to $CDCl_3$, $[Au(PPh_3)NTf_2]$ was added and the mixture heated to 60 °C for 4–48 h while monitored by NMR spectroscopy. After workup, **4b–6b** were isolated in yields of 64–72% over both steps (Scheme 3).

The boronic acid **7a** turned out to be a special case: although a double cyclization reaction is possible and affords the B,O_2-PAH **8a** in 86% yield, it requires a reaction time of several hours rather than minutes at room temperature (Scheme 4).

Even upon heating of **7a** with 2.5 equiv. of $(Me_3Si)_2NMe$, the amination reaction stopped at the stage of the methylamino(hydroxy)borane **7b** (Scheme 4); for the subsequent targeted synthesis of **7b**, 1.5 equiv. of $(Me_3Si)_2NMe$ were used (C_6D_6, 120 °C, 2–3 d). Treatment of **7b** with 2–25 mol% of $[Au(PPh_3)NTf_2]$ resulted in a 6-*endo*-dig addition of the BN–H bond across the C≡C bond (60 °C, 4–48 h; **8c**), whereas no B,O-doped ring was formed; the optimized protocol for the synthesis of **8c** uses 2 mol% $[Au(PPh_3)NTf_2]$ and a reaction time of 4 h. The complete cyclization of **8c** to the B,N,O-phenalenyl **8ab** was finally achieved by addition of F_3CSO_3H (TfOH).[87,88]

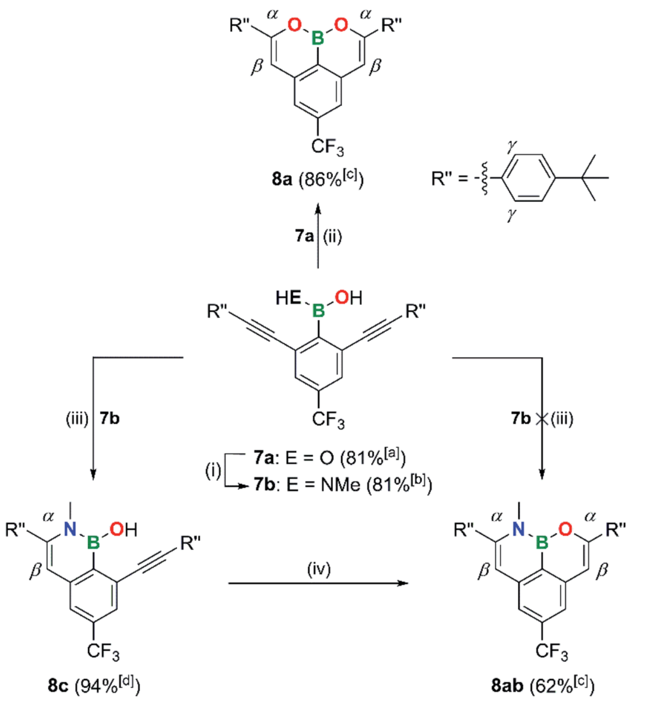

Scheme 4 Synthesis of compounds **8a–c**. Reagents and conditions: (i) 1.5 equiv. $(Me_3Si)_2NMe$, C_6D_6, 120 °C, 2–3 d, sealed NMR tube. (ii) 1 mol% $[Au(PPh_3)NTf_2]$, $CHCl_3$, room temperature, 4–6 h. (iii) 2 mol% $[Au(PPh_3)NTf_2]$, $CDCl_3$, 60 °C, 4 h. (iv) 5 drops TfOH (approx. 1 equiv.), CH_2Cl_2, room temperature, 5 min. [a] Yield over three steps from commercially available chemicals. [b] Yield over four steps from commercially available chemicals. [c] Yield of the final cyclization step. [d] Yield of the final cyclization step without isolation of **7b**.

These results are remarkable in several respects: (i) **8ab** is the first B,N,O-PAH available so far. (ii) When the reactions are independent, the ring closure to the $(B,O)_n$-PAHs with the $[Au(PPh_3)NTf_2]$ catalyst is generally faster than the formation of the corresponding $(B,N)_n$-PAHs. However, for **7b**, when there is now intramolecular competition between N–H and O–H, cyclization to the B,N heterocycle is preferred.[89] (iii) TfOH can also be a suitable cyclization catalyst and in this particular example it is even superior to $[Au(PPh_3)NTf_2]$.

The closest relatives of our B,O-naphthalene **4a** are Sheppard's boron enolates shown in Scheme 2b.[43] Some of these derivatives (*e.g.*, R″ = H,[45] *n*Bu[43]) were characterized by NMR spectroscopy, IR spectroscopy, and high resolution mass spectrometry. The optoelectronic properties were not investigated. Yet, the presence of a strongly π-donating OH substituent at the B atom of Sheppard's enolates should lead to a lesser extent of double bonding in the endocyclic B–O bond than in the case of **4a**, which carries an electronically more innocent Mes substituent.[90] A doubly benzannulated congener of the B,O_2-doped phenalenyl **8a** was prepared by Hatakeyama *via* demethylative direct borylation of 2,2″-dimethoxy-1,1′:3′,1″-terphenyl (BBr_3/TMP, 180 °C, 18 h; TMP = 2,2,6,6-tetramethylpiperidine; see Scheme 2a for a related reaction).[31] No precedence exists for the B,O- and $(B,O)_2$-anthracenes **5a** and **6a**.

Fig. 1 shows the sequence of relative thermodynamic stabilities of all conceivable parental B,N-naphthalene isomers according to quantum-chemical calculations (R^1–R^8 = H);[91] substitution has been achieved at the indicated positions. We note that the energetically favorable 2,1-B,N- and 1,2-B,N-naphthalenes differ from the other known isomers by the presence of unperturbed aromatic C_6 rings.[3]

The most stable 2,1-B,N-naphthalenes are also by far the most thoroughly studied isomers.[18,19,92–103] The dominant synthesis strategies rely on ring-closing reactions between *o*-vinyl-/*o*-alkynylanilines and $R'BCl_2$ or $K[R'BF_3]/SiCl_4/NEt_3$ (*cf.* Scheme 1a; R′ = halogen, alkyl, alkenyl, alkynyl, (hetero)-aryl).[18,19,92,93,95,99,102] An "aromatic metamorphosis" approach (*cf.* Scheme 2c) is based on reductive ring opening of indoles with excess Li metal, trapping of the dilithiated intermediate with RBpin, and aqueous workup.[103]

Apart from our current work on the second most stable 1,2-B,N-naphthalenes, the only other report comes from the Cui group.[104] They used benzylic imines as key intermediates (3 synthesis steps) and converted them into the corresponding enamidyl dibromoboranes, which were cyclized *via* an Et_3N-promoted intramolecular electrophilic aromatic borylation reaction at 80 °C (2 steps; yields: 30–51% with respect to the corresponding benzylic imine). The authors demonstrated a scope of their reaction sequence across the substituents R^1 = alkynyl/(hetero)aryl, R^2 = aryl, R^3 = *t*Bu/Ph, R^5 = F and R^6 = Me.

Apart from the B,N-anthracenes **5b** and **6b**, their orientational isomers 2,1-B,N-anthracene and 2,6-B_2-1,5-N_2-anthracene are known. The air-stable compounds are accessible through

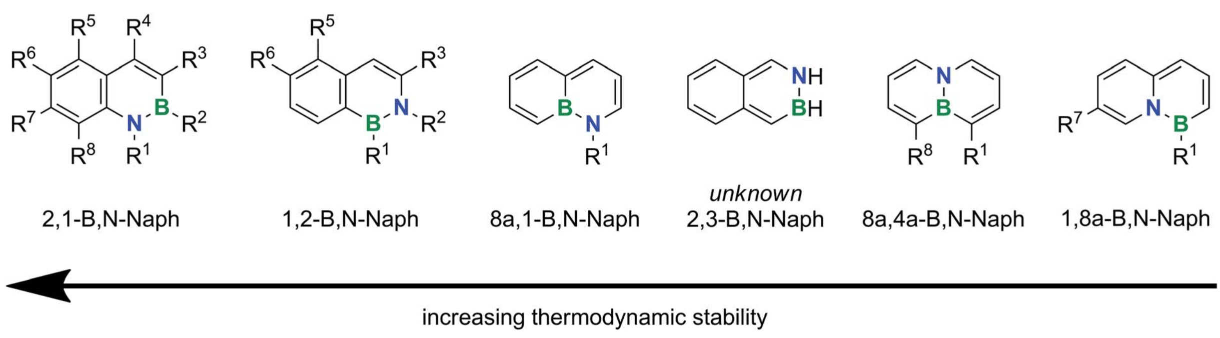

Fig. 1 Relative thermodynamic stabilities of B,N isosters of naphthalene containing one B,N unit. Substitutions have been achieved at the indicated positions.

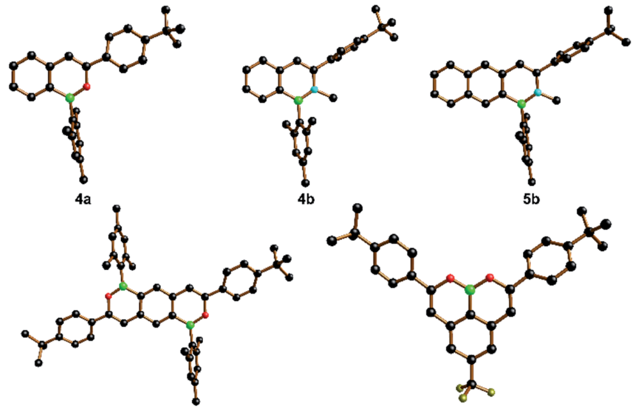

Fig. 2 Crystallographically determined solid-state structures of **4a**, **4b**, **5b**, **6a**, and **8a**; H atoms were omitted for clarity. Selected bond lengths [Å] and dihedral angles [°]: **4a**: B–O = 1.388(2), C(α)–C(β) = 1.345(2); BO ring//mesityl = 83.1(1), BO ring//tBuC$_6$H$_4$ = 17.0(1). **4b**: B–N = 1.417(5), C(α)–C(β) = 1.356(6); BN ring//mesityl = 78.0(1), BN ring//tBuC$_6$H$_4$ = 83.0(1). **5b**: B–N = 1.435(7), C(α)–C(β) = 1.328(7); BN ring//mesityl = 85.3(2), BN ring//tBuC$_6$H$_4$ = 82.1(2). **6a**: B–O = 1.374(3), C(α)–C(β) = 1.340(3); BO ring//mesityl = 75.7(1), BO ring//tBuC$_6$H$_4$ = 28.3(1). **8a**: B–O = 1.368(4)/1.381(5), C(α)–C(β) = 1.344(5)/1.345(4); BO ring//tBuC$_6$H$_4$ = 14.4(2)/33.6(1).

(double) borylative cyclization of 2-amino-3-vinylnaphthalene or 1,4-diamino-2,5-divinylbenzene with BCl$_3$. Subsequent Cl/H exchange using LiAlH$_4$ afforded the target molecules in about 80% yield over the last two steps.[79]

To conclude, our novel synthesis approach for (B,N)$_n$- and (B,O)$_n$-doped PAHs (i) provides previously inaccessible positional isomers in yields competitive with any alternative cyclization reaction developed to-date, (ii) is modular, as it allows the synthesis of (B,E)$_n$ derivatives with E = N and O starting from the same late precursors, and (iii) takes advantage of well-established borinic and boronic acid chemistry, avoiding the use of corrosive, air- and moisture-sensitive haloboranes.

NMR-spectroscopic and X-ray crystallographic characterization of 4a,b–6a,b and 8a–c

All spectra were run in CDCl$_3$.[105] In the ^{1}H NMR spectra of **4a,b–6a,b** and **8a–c**, the successful cyclization reactions are indicated by the presence of singlet resonances in the aromatic regions, which are due to the newly generated H$^\beta$ protons (see Schemes 3 and 4 for the position labels). The ^{13}C{^{1}H} NMR spectra of **4a,b–6a,b** no longer contain signals characteristic of C(sp) atoms; instead, new resonances appear that belong to C$^\beta$ (**4a–6a**: av. 106.2 ppm; **4b–6b**: av. 113.4 ppm) and C$^\alpha$ (**4a–6a**: av. 151.8 ppm; **4b–6b**: av. 145.7 ppm). Intense cross peaks between the NCH_3 proton signals and the C$^\alpha$ signals are observed in all ^{H,C}HMBC spectra of **4b–6b**. The ^{11}B NMR shift values of **4a,b–6a,b** are found in the expected region of 39–46 ppm.[106]

The B,O$_2$-phenalenyl **8a** shows NMR features similar to those of the B,O-naphthalene **4a** (**8a:** δ(H$^\beta$) = 6.97, δ(C$^\beta$) = 104.2, δ(C$^\alpha$) = 154.2), but its ^{11}B signal is significantly shifted to higher field as a result of better magnetic shielding by the two π-donating O atoms (**8a:** 29 ppm *vs.* **4a:** 46 ppm). For the singly ring-closed compound **8c**, we observe simultaneously resonances attributable to CH$^\beta$ and C$^\alpha$ units and those attributable to two alkynyl-C atoms. An ^{H,C}HMBC experiment proved the formation of a 1,2-B,N-naphthalene core with dangling OH substituent (δ(OH) = 7.14). The ^{1}H NMR spectrum of the B,N,O-phenylene **8ab**, in contrast, lacks an OH signal and instead shows two well-resolved H$^\beta$ resonances at 6.34 and 6.89 ppm. While two C$^\beta$ resonances appear at 104.2 and 108.1 ppm, alkynyl-C signals are not detectable in the ^{13}C{^{1}H} NMR spectrum of **8ab**.

Further comparison of the NMR spectra of **4a–6a** on the one hand and **4b–6b** on the other reveals additional remarkable differences in the molecular and electronic structures as a function of B,O- *vs.* B,N-doping. While the ^{1}H and ^{13}C chemical shift values of the Mes substituents are largely the same, especially the CH$^\gamma$ values of the tBuC$_6$H$_4$ groups of **4a–6a** (δ(H$^\gamma$) = av. 7.94 ppm; δ(C$^\gamma$) = av. 125.2 ppm) are significantly different from those of **4b–6b** (δ(H$^\gamma$) = av. 7.39 ppm; δ(C$^\gamma$) = av. 129.1 ppm). The same is true for the B,O-half of **8ab** (δ(H$^\gamma$) = 7.87 ppm; δ(C$^\gamma$) = 125.3 ppm) compared to its B,N-half (δ(H$^\gamma$) = 7.36 ppm; δ(C$^\gamma$) = 128.9 ppm). These differences can be explained by different conformations of the tBuC$_6$H$_4$ substituents with respect to the heterocyclic cores in **4a,b–6a,b**: the small O atom allows an essentially coplanar arrangement in solution, whereas the larger NMe group enforces a twist between the two moieties (the bulky Mes rings are consistently orthogonally positioned). Different conformations between **4a–6a** and **4b–6b** are also observed in the solid state and are relevant for the interpretation of the optoelectronic properties of the B,O- *vs.* B,N-doped species (see below).

Looking at **4a,b/5a,b**, we find that the C$^\varepsilon$ atoms are deshielded by about 10 ppm with respect to the C$^\delta$ atoms, regardless of whether the compounds contain O or N atoms (δ(C$^\delta$) = 126.4 (**4a**), 126.1 (**4b**), 124.0 (**5a**), 123.4 ppm (**5b**); δ(C$^\varepsilon$) = 136.5 (**4a**), 135.5 (**4b**), 138.9 (**5a**), 136.8 ppm (**5b**)). Given that the δ(C$^\delta$) values are close to that of C$_6$H$_6$ (128.4 ppm), the +M effect of O and N does not seem to reach out to this position, whereas the π-charge density at C$^\varepsilon$ is apparently reduced due to the −M effect of B. In line with this interpretation, the two equivalent CH atoms of the benzene cores of **6a,b**, which should experience the ±M effects of both dopant elements, are also considerably deshielded (134.7 (**6a**), 133.2 ppm (**6b**)). We also note that plots of the highest occupied molecular orbitals (HOMOs) of **4a,b/5a,b** consistently indicate a larger contribution of the p$_z$ orbital located at C$^\delta$ than of the p$_z$ orbital located at C$^\varepsilon$ (see the ESI†).

The product molecules **4a**, **6a**, **8a** and **4b**, **5b** have been characterized by X-ray crystallography (Fig. 2; the solid-state structures of numerous intermediates are compiled in the ESI†). As a general feature, the B–O distances (1.368(4)–1.388(2) Å) are significantly shorter than the B–N distances (1.417(5)–1.435(7) Å), and this is even true for the boronic acid ester **8a**, in which two π-donating O atoms compete for the same p$_z$(B) acceptor orbital. Apart from different grades of $^-$B=E$^+$ double-bond character (E = O, N), other influencing factors are the smaller covalent radius of the O atom compared to the N atom (which also carries a Me substituent here) and a lower degree of intramolecular steric repulsion in the B,O-doped compounds. In agreement with this latter factor and the NMR data discussed above, we find much

Table 1 Photophysical, electrochemical, and computational data of the compounds **5a,b–6a,b** and **8a**, **8ab**. Optical measurements were performed in $CHCl_3$, and electrochemical measurements were performed in THF (room temperature, supporting electrolyte: $[nBu_4N][PF_6]$ (0.1 M), scan rate: 200 mV s^{-1})

	λ_{abs} [nm] (ε [M^{-1} cm^{-1}])	λ_{onset}[a] [nm]	λ_{em}[b] [nm]	Φ_{PL}[c] [%]	E_G^{opt}[d] [eV]	E'^{DFT}_G[e] [eV]	$E_{1/2}$ [V]	E^{CV}_{LUMO}[f] [eV]	E'^{DFT}_{LUMO}[g] [eV]	E'^{DFT}_{HOMO}[h] [eV]
5a	290 (45 925) 297 (45 316) 328 (sh) 339 (34 508) 351 (20 644) 379 (sh) 395 (sh)	419	426 (sh) 445	20 31[i]	2.96	2.87	−2.58	−2.22	−2.23	−5.10
5b	268 (44 824) 326 (9621) 341 (12 571) 379 (sh) 405 (sh)	422	428 (sh) 448 470 (sh)	32 51[i]	2.94	2.93	−2.80	−2.00	−2.03	−4.96
6a	312 (sh) 326 (sh) 343 (sh) 360 (75 215) 373 (56 253) 404 (13 108) 425 (8628)	447	452 475 507 (sh)	41 49[i]	2.77	2.73	—	—	−2.27	−5.00
6b	347 (27 027) 388 (sh)	422	426 446	16 52[i]	2.94	2.98	−3.00	−1.80	−1.80	−4.78
8a	270 (13 015) 314 (25 351) 329 (sh) 366 (5963) 386 (4312)	399	397 419 443 468 510 (sh)	43 52[i]	3.11	3.02	—	—	−2.20	−5.22
8ab	307 (30 228) 315 (sh) 329 (27 393) 374 (10 481) 393 (sh)	412	398 (sh) 415 434 461 (sh) 491 (sh)	34 44[i]	3.01	2.98	—	—	−2.03	−5.01

[a] Each onset wavelength (λ_{onset}) was determined by constructing a tangent on the point of inflection of the bathochromic slope of the most red-shifted absorption maximum. [b] Resolved vibrational fine structure. [c] Quantum yields were determined by using a calibrated integrating sphere. [d] Optical band gap $E_G^{opt} = 1240/\lambda_{onset}$. [e] For better comparability with the E_G^{opt} values, the computed energy gaps (E_G^{DFT}) have been scaled according to the following linear equation: $E'^{DFT}_G = 0.65 \times E^{DFT}_G + 0.48$. [f] $E^{CV}_{LUMO} = -4.8 \text{ eV} - E_{1/2}$ ($FcH/FcH^+ = -4.8$ eV *vs.* vacuum level). [g] For better comparability with the E^{CV}_{LUMO} values, the computed LUMO energies (E^{DFT}_{LUMO}) have been scaled according to the following linear equation: $E'^{DFT}_{LUMO} = 0.65 \times E^{DFT}_{LUMO} - 1.20$. [h] Scaled HOMO energies (E'^{DFT}_{HOMO}) were calculated from the scaled LUMO energies (E'^{DFT}_{LUMO}) and the scaled HOMO–LUMO energy gaps ($E'^{DFT}_{HOMO} = E'^{DFT}_{LUMO} - E'^{DFT}_G$). [i] Quantum yields measured in *c*-hexane. sh = shoulder.

smaller dihedral angles between the B,O heterocycles and the $tBuC_6H_4$ substituents in **4a**, **6a**, **8a** (14.4(2)–33.6(1)°) than between the B,N heterocycles and the $tBuC_6H_4$ ring in **4b**, **5b** (82.1(2)–83.0(1)°).

A comparison of the C–C distances in **4a**, **6a**, **8a** and **4b**, **5b** also provides insight into the degree of cyclic π-delocalization along the molecules' cores: all C^α–C^β distances fall in the range 1.328(7)–1.356(6) Å, which is indicative for largely isolated C^α═C^β double bonds (ideal value: 1.34 Å).[107] The adjacent C^β–Ar distances, in turn, are consistently longer (1.437(6)–1.447(7) Å) than C^α═C^β and also longer than all C–C distances in the annulated benzene rings. Taken together, these data point toward Clar's sextets in the carbonaceous six-membered rings and attached –B═E–C═C– heterobutadiene fragments. We finally note that the $^-$B═N^+ bond lengths found in our 1,2-B,N-naphthalene **4b** and 1,2-B,N-anthracene **5b** do not differ from those in corresponding 2,1-B,N-naphthalenes/anthracenes and are thus not influenced by the orientation of the B,N pairs.[95,96,108]

Optoelectronic properties of 4a,b–6a,b and 8a, 8ab

Of the newly synthesized B,O- and B,N-PAHs compiled in Schemes 3 and 4, only the B,E-anthracenes **5a,b** and the $(B,N)_2$-anthracene **6b** show (quasi)reversible redox waves in their cyclic voltammograms (*vs.* FcH/FcH^+; THF, room temperature, supporting electrolyte: 0.1 M $[nBu_4N][PF_6]$; Table 1). **5a** ($E_{1/2} = -2.58$ V) is easier to reduce by 220 mV than **5b** ($E_{1/2} = -2.80$ V), likely due to the higher electronegativity of the O atom compared to the N atom and the extension of the conjugation pathway into the coplanar $tBuC_6H_4$ ring (*cf.* the conformations adopted by **4a** *vs.* **4b** in the solid state; Fig. 2). For a comparable 2,1-B,N-anthracene bearing a mesityl group on boron as the sole substituent, a peak cathodic potential of $E_{p,c} = -2.59$ V (DMF) was reported.[108] These data indicate that the electrochemical properties of the B,E-anthracenes are not only influenced by the choice of E = N or O but also by subtle effects resulting from the orientation of the introduced B,E pairs.[12] Reduction of the

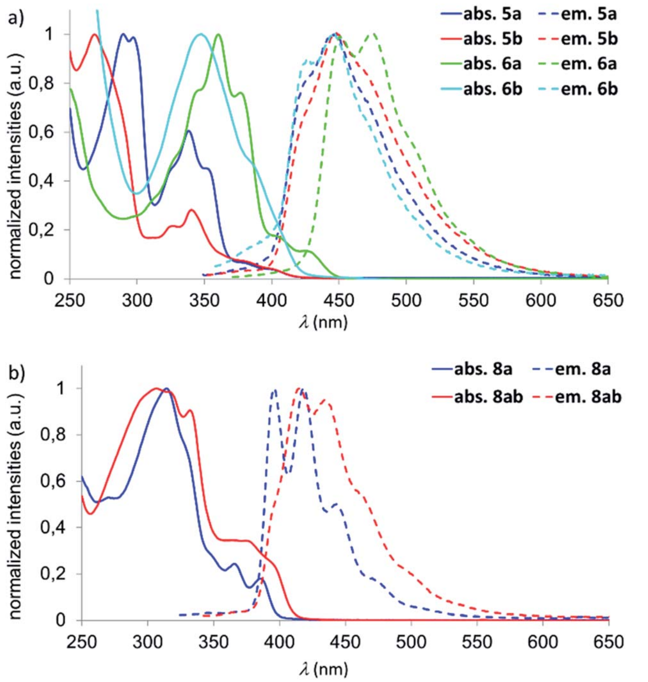

Fig. 3 (a) Normalized UV/vis absorption (solid lines) and emission (dashed lines) spectra in $CHCl_3$ of compounds **5a,b–6a,b**. (b) Normalized UV/vis absorption (solid lines) and emission (dashed lines) spectra in $CHCl_3$ of compounds **8a** and **8ab**.

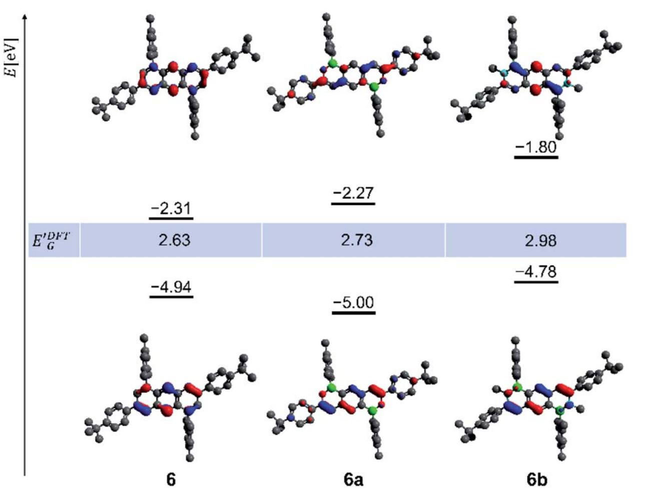

Fig. 4 DFT-calculated nodal structures and scaled energy levels of the frontier orbitals of the parental 1,5-dimesityl-3,7-di(tBuC$_6$H$_4$)anthracene (**6**), **6a**, and **6b** (HOMOs bottom, LUMOs top; isovalue of the isosurface plots: 0.05 $a_0^{-3/2}$; B3LYP/6-31G*).

$(B,N)_2$-anthracene **6b** occurs at $E_{1/2} = -3.00$ V and is thus somewhat harder to achieve than the reduction of the B,N-anthracene **5b** ($E_{1/2} = -2.80$ V).

UV/vis spectra were recorded for **4a,b–6a,b** and **8a**, **8ab** ($CHCl_3$); photoluminescence spectra of these compounds were measured both in $CHCl_3$ and *c*-hexane (Fig. 3 and Table 1). The naphthalene derivatives **4a,b** show low photoluminescence quantum efficiencies of $\Phi_{PL} < 10\%$ and will therefore not be discussed further. We first focus on the onsets of absorbance (λ_{onset}), since these are directly correlated with the HOMO–LUMO energy gaps (E_G^{opt}). The λ_{onset} values of **5a**/**5b** (419/422 nm) are almost identical, which is also true for the emission wavelengths λ_{em} (426/428 nm). Thus, despite their different LUMO levels, E_G^{opt} is the same for the two B,E-anthracenes. In contrast, both the onset of absorbance and the emission wavelength are bathochromically shifted for **6a** compared to **6b** ($\lambda_{onset} = 447$ *vs.* 422 nm; $\lambda_{em} = 452$ *vs.* 426 nm). Here, the impact of two *vs.* zero coplanar tBuC$_6$H$_4$ substituents and an associated enlarged π-electron system in **6a** may play a role.

If recorded in *c*-hexane, all emissions are detected at somewhat shorter wavelengths compared to measurements in $CHCl_3$ ($\Delta(\lambda_{em})$ = 260–920 cm^{-1}), the vibrational fine structures are even better resolved, and quantum efficiencies of $\Phi_{PL} = 31\%$ (**5a**), 51% (**5b**), 49% (**6a**), and 52% (**6b**) are obtained. The trends in the experimentally determined optical band gaps E_G^{opt}(**5a**) ≈ E_G^{opt}(**5b**) ≈ E_G^{opt}(**6b**) > E_G^{opt}(**6a**) are well reproduced by quantum-chemical calculations (*cf.* the scaled values E'^{DFT}_G in Table 1). The calculations also confirm a less cathodic reduction potential of **5a** compared to **5b**, reflected by the lower computed LUMO energy of **5a**.

The gas-phase structures and frontier-orbital configurations of **6a**/**6b** and their carbonaceous congener **6** are exemplarily shown in Fig. 4. Orthogonally positioned Mes rings are seen throughout, while the tBuC$_6$H$_4$ substituents in **6a** are less twisted with respect to the heterocyclic core than in **6b**, which agrees well with the X-ray crystallography results (Fig. 2). Compound **6** possesses a smaller energy gap $E'^{DFT}_G = 2.63$ eV than **6a** (2.73 eV) and **6b** (2.98 eV). As an important difference between our B,N-anthracenes **5b**/**6b** and Liu's positional isomers 2,1-B,N-anthracene and 2,6-B$_2$-1,5-N$_2$-anthracene, the π systems of the C$^\alpha$=C$^\beta$ bonds contribute strongly to the HOMOs of the former compounds (Fig. 4) but only negligibly to those of the latter.[79]

The optical properties of the B,O$_2$- and B,N,O-phenalenyls are similar and therefore do not require further discussion (Table 1 and Fig. 3b). However, we note pleasingly high photoluminescence quantum efficiencies of $\Phi_{PL} = 52\%$ (**8a**) and 44% (**8ab**) in *c*-hexane.

Late-stage derivatization of the (B,O)$_2$-perylene 9

With increasing knowledge about B,N-PAHs it becomes more and more obvious that functional groups do not necessarily have to be introduced before the cyclization step. Late stage derivatization, a widely used tool in PAH chemistry, is also possible and often remarkably regioselective (see corresponding reactions on 2,1-B,N-benzenes and 2,1-B,N-naphthalenes).[16] Given the higher reactivity of B,O- compared to B,N-PAHs (see above), we were interested in exploring whether late-stage functionalizations of the former are also possible, while maintaining the structural integrity of the heterocyclic scaffold. For this purpose, we selected the parent (B,O)$_2$-perylene **9** (Scheme 5), which allows a direct comparison with its highly symmetric carbonaceous counterpart. As functional group to be introduced, the pinacolatoboryl (Bpin) substituent was chosen.

Similar to other (B,O)$_2$-perylenes,[55] compound **9** was synthesized by double cyclization of the diethynylated 9,10-

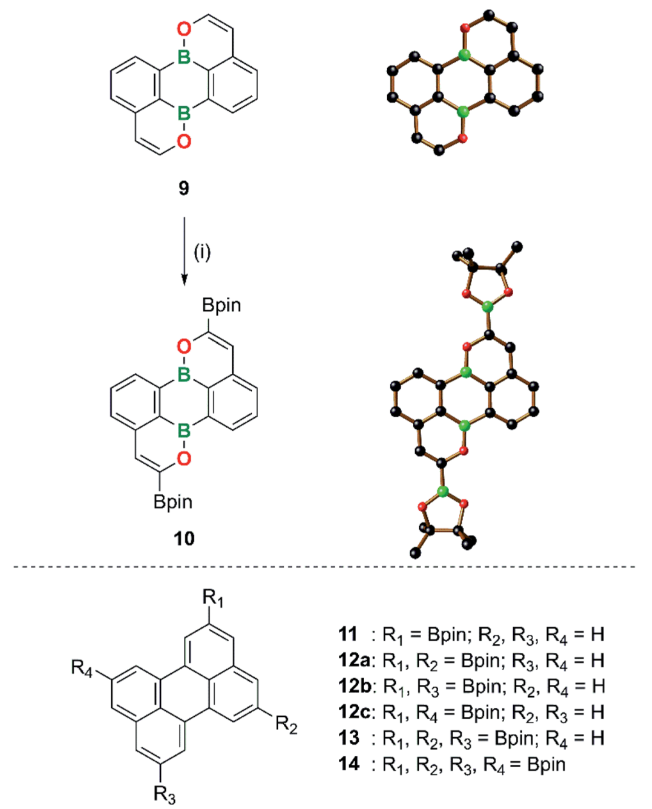

Scheme 5 Transformation of $(B,O)_2$-perylene **9** to the doubly Bpin-substituted $(B,O)_2$-perylene **10** by Ir-catalyzed borylation and their structures in the solid state. Reagents and conditions: (i) 3.1 equiv. B_2pin_2, 3 mol% $[Ir(COD)(\mu\text{-}OMe)]_2$, 6 mol% dtbpy, THF, 80 °C, 42 h.

dihydroxy-9,10-dihydro-9,10-diboraanthracene derivative using the $[Au(PPh_3)NTf_2]$ catalyst (Scheme 5).[109] The successful preparation of **9** thus demonstrates the applicability of our method to substrates carrying terminal alkynes (see the ESI† for full details). Treatment of **9** with 3.1 equiv. of B_2pin_2 in the presence of the catalyst system 1/2 $[Ir(COD)(\mu\text{-}OMe)]_2$/dtbpy[110–112] led to a quantitative (TLC) double C–H borylation at the two C atoms in α-position to the O atoms and gave the corresponding product **10** in 63% yield after workup (Scheme 5; COD = 1,5-cyclooctadiene, dtbpy = 4,4′-di-*tert*-butyl-2,2′-bipyridine). No mono-, tri-, or tetraborylated derivatives were observed; an increase in the amount of added B_2pin_2 to 5 equiv. did not lead to higher borylation levels either. The regioselectivity of the functionalization reaction was confirmed by X-ray crystallography (Scheme 5) and NMR spectroscopy. **10** gives rise to two resonances in the ^{11}B NMR spectrum and four resonances in the aromatic region of the ^{1}H NMR spectrum. Three doublets of doublets (each integrating 2H) can be assigned to the C_6H_3 fragments and the remaining singlet (2H) to the protons at the positions β to the O atoms (^{H,C}HMBC experiment).

The regioselectivity of the borylation of **9** is based on two factors: (i) the key intermediate of the catalytic cycle, *fac*-$[Ir(dtbpy)(Bpin)_3]$, is a rather bulky metal complex that avoids performing the rate-determining C–H-activation step at sterically encumbered positions *ortho* to ring junctions or other substituents.[113,114] Activation of the *peri*-C–H bonds of **9** (or perylene) is therefore unfavorable. (ii) Of the four remaining C–H bonds, the two adjacent to the electronegative O atom, which is also smaller than a neighboring C–H unit, react preferentially.[115] In contrast to the selective diborylation of **9**, the corresponding reaction between carbonaceous perylene and 2.2 equiv. of B_2pin_2 furnished a mixture of mono- (**11**), di- (three isomers, **12a–c**), tri- (**13**), and tetraborylated (**14**) products (Scheme 5). While the perylenes carrying different numbers of Bpin substituents have been separated by HPLC, it has been found impossible to separate **12a–c**. On the other hand, the 2,5,8,11-tetraborylated perylene **14**, which does not (yet) have a $(B,O)_2$-analogue, was accessible in 83% yield by using 4.4 equiv. of B_2pin_2 and the Ir catalyst (Scheme 5).[114,116–118]

Conclusions

We have shown that the mild Au(I)-mediated cyclization of aryl(amino)boranes or aryl boronic and borinic acids with *ortho*-positioned C≡C bonds is an ideal tool for the synthesis of singly and doubly B,N- or B,O-doped polycyclic aromatic hydrocarbons (PAHs). We see the following advantages of this new method over many of the existing protocols: (i) boronic and borinic acids, which are nowadays standard reagents in every synthesis-oriented laboratory, serve as starting materials. (ii) The use of sophisticated organometallic reagents or corrosive boron halides is avoided. (iii) Modularity is achieved by the fact that the aminoboranes required for the synthesis of the B,N-PAHs are accessible in one step from the boronic and borinic acids required for the fabrication of the B,O-PAHs. The cyclization protocols presented herein thus represent a significant addition to the currently available toolbox for doping PAHs with main-group elements. Moreover, by using an unsubstituted $(B,O)_2$-perylene as the substrate for Ir-catalyzed C–H borylation, we (i) present a rare example of late-stage functionalization of a B,O-PAH and (ii) show that the exchange of two C═C for $^{-}B{=}O^{+}$ bonds leads to dramatically improved product selectivity compared to the case of the carbonaceous perylene.

Author contributions

T. K. performed the late-stage derivatization of compound **9**; O. O. synthesized and characterized all other compounds. M. B. performed the X-ray crystal structure analyses. H.-W. L. and M. W. supervised the project. The manuscript was written by M. W. and O. O. and edited by all the co-authors.

Conflicts of interest

There are no conflicts to declare.

Acknowledgements

We gratefully acknowledge Aleksandar Lucic for his assistance with manuscript preparation.

Notes and references

1 (*a*) *Main Group Strategies towards Functional Hybrid Materials*, ed. T. Baumgartner and F. Jäkle, John Wiley & Sons, Ltd., Chichester, UK, 1st edn, 2017; (*b*) S. E. Prey and M. Wagner, *Adv. Synth. Catal.*, 2021, **363**, DOI: 10.1002/adsc.202001356; (*c*) S. K. Mellerup and S. Wang, *Trends Chem.*, 2019, **1**, 77–89; (*d*) E. von Grotthuss, A. John, T. Kaese and M. Wagner, *Asian J. Org. Chem.*, 2018, **7**, 37–53; (*e*) M. Stępień, E. Gońka, M. Żyła and N. Sprutta, *Chem. Rev.*, 2017, **117**, 3479–3716; (*f*) L. Ji, S. Griesbeck and T. B. Marder, *Chem. Sci.*, 2017, **8**, 846–863; (*g*) S. Yamaguchi, A. Fukazawa and M. Taki, *J. Synth. Org. Chem.*, 2017, **75**, 1179–1187; (*h*) P. Zhao, D. O. Nettleton, R. G. Karki, F. J. Zécri and S. Y. Liu, *ChemMedChem*, 2017, **12**, 358–361; (*i*) L. Schweighauser and H. A. Wegner, *Chem.–Eur. J.*, 2016, **22**, 14094–14103; (*j*) A. Escande and M. J. Ingleson, *Chem. Commun.*, 2015, **51**, 6257–6274; (*k*) A. Wakamiya and S. Yamaguchi, *Bull. Chem. Soc. Jpn.*, 2015, **88**, 1357–1377; (*l*) J. Kahlert, C. J. D. Austin, M. Kassiou and L. M. Rendina, *Aust. J. Chem.*, 2013, **66**, 1118–1123; (*m*) B. C. Das, P. Thapa, R. Karki, C. Schinke, S. Das, S. Kambhampati, S. K. Banerjee, P. van Veldhuizen, A. Verma, L. M. Weiss and T. Evans, *Future Med. Chem.*, 2013, **5**, 653–676; (*n*) F. Issa, M. Kassiou and L. M. Rendina, *Chem. Rev.*, 2011, **111**, 5701–5722; (*o*) S. J. Baker, C. Z. Ding, T. Akama, Y.-K. Zhang, V. Hernandez and Y. Xia, *Future Med. Chem.*, 2009, **1**, 1275–1288.

2 (*a*) Z. X. Giustra and S.-Y. Liu, *J. Am. Chem. Soc.*, 2018, **140**, 1184–1194; (*b*) J. Huang and Y. Li, *Front. Chem.*, 2018, **6**, 1–22; (*c*) G. Bélanger-Chabot, H. Braunschweig and D. K. Roy, *Eur. J. Inorg. Chem.*, 2017, **2017**, 4353–4368; (*d*) H. Helten, *Chem.–Eur. J.*, 2016, **22**, 12972–12982; (*e*) X.-Y. Wang, J.-Y. Wang and J. Pei, *Chem.–Eur. J.*, 2015, **21**, 3528–3539; (*f*) P. G. Campbell, A. J. V. Marwitz and S.-Y. Liu, *Angew. Chem., Int. Ed.*, 2012, **51**, 6074–6092; (*g*) M. J. D. Bosdet and W. E. Piers, *Can. J. Chem.*, 2009, **87**, 8–29; (*h*) Z. Liu and T. B. Marder, *Angew. Chem., Int. Ed.*, 2008, **47**, 242–244. For selected B- and N-doped polycyclic aromatic hydrocarbons that are devoid of direct $^{-}B{=}N^{+}$ bonds and show exciting optoelectronic properties, see: (*i*) T. Hatakeyama, K. Shiren, K. Nakajima, S. Nomura, S. Nakatsuka, K. Kinoshita, J. Ni, Y. Ono and T. Ikuta, *Adv. Mater.*, 2016, **28**, 2777–2781; (*j*) S. Nakatsuka, H. Gotoh, K. Kinoshita, N. Yasuda and T. Hatakeyama, *Angew. Chem., Int. Ed.*, 2017, **56**, 5087–5090; (*k*) X. Liang, Z.-P. Yan, H.-B. Han, Z.-G. Wu, Y.-X. Zheng, H. Meng, J.-L. Zuo and W. Huang, *Angew. Chem., Int. Ed.*, 2018, **57**, 11316–11320; (*l*) K. Matsui, S. Oda, K. Yoshiura, K. Nakajima, N. Yasuda and T. Hatakeyama, *J. Am. Chem. Soc.*, 2018, **140**, 1195–1198; (*m*) Y. Kondo, K. Yoshiura, S. Kitera, H. Nishi, S. Oda, H. Gotoh, Y. Sasada, M. Yanai and T. Hatakeyama, *Nat. Photonics*, 2019, **13**, 678–682.

3 Various numbering schemes have been used in the literature to indicate the positions (x,y) and orientations of the B,E pairs in x,y-B,E-doped PAHs (E = N, O). In this publication, we use the conventional IUPAC scheme for numbering the C atoms in the parental carbonaceous PAHs. We will also always name the B atom first and adapt the sequence of the numbers x and y in the compounds' names accordingly (see Fig. 1).

4 C. A. Jaska, D. J. H. Emslie, M. J. D. Bosdet, W. E. Piers, T. S. Sorensen and M. Parvez, *J. Am. Chem. Soc.*, 2006, **128**, 10885–10896.

5 M. J. D. Bosdet, W. E. Piers, T. S. Sorensen and M. Parvez, *Angew. Chem., Int. Ed.*, 2007, **46**, 4940–4943.

6 M. J. D. Bosdet, C. A. Jaska, W. E. Piers, T. S. Sorensen and M. Parvez, *Org. Lett.*, 2007, **9**, 1395–1398.

7 A. J. V. Marwitz, M. H. Matus, L. N. Zakharov, D. A. Dixon and S.-Y. Liu, *Angew. Chem., Int. Ed.*, 2009, **48**, 973–977.

8 A. Chrostowska, S. Xu, A. N. Lamm, A. Mazière, C. D. Weber, A. Dargelos, P. Baylère, A. Graciaa and S.-Y. Liu, *J. Am. Chem. Soc.*, 2012, **134**, 10279–10285.

9 B. Neue, J. F. Araneda, W. E. Piers and M. Parvez, *Angew. Chem., Int. Ed.*, 2013, **52**, 9966–9969.

10 E. R. Abbey, A. N. Lamm, A. W. Baggett, L. N. Zakharov and S.-Y. Liu, *J. Am. Chem. Soc.*, 2013, **135**, 12908–12913.

11 X. Y. Wang, A. Narita, X. Feng and K. Müllen, *J. Am. Chem. Soc.*, 2015, **137**, 7668–7671.

12 J. S. A. Ishibashi, A. Dargelos, C. Darrigan, A. Chrostowska and S.-Y. Liu, *Organometallics*, 2017, **36**, 2494–2497.

13 H. Lin, C. R. McConnell, B. Jilus, S.-Y. Liu and F. Jäkle, *Macromolecules*, 2019, **52**, 4500–4509.

14 A. S. Scholz, J. G. Massoth, M. Bursch, J.-M. Mewes, T. Hetzke, B. Wolf, M. Bolte, H.-W. Lerner, S. Grimme and M. Wagner, *J. Am. Chem. Soc.*, 2020, **142**, 11072–11083.

15 M. Chen, K. S. Unikela, R. Ramalakshmi, B. Li, C. Darrigan, A. Chrostowska and S.-Y. Liu, *Angew. Chem., Int. Ed.*, 2021, **60**, 1556–1560.

16 C. R. McConnell and S.-Y. Liu, *Chem. Soc. Rev.*, 2019, **48**, 3436–3453.

17 T. Hatakeyama, S. Hashimoto, T. Oba and M. Nakamura, *J. Am. Chem. Soc.*, 2012, **134**, 19600–19603.

18 S. R. Wisniewski, C. L. Guenther, O. A. Argintaru and G. A. Molander, *J. Org. Chem.*, 2014, **79**, 365–378.

19 F.-D. Zhuang, J.-M. Han, S. Tang, J.-H. Yang, Q.-R. Chen, J.-Y. Wang and J. Pei, *Organometallics*, 2017, **36**, 2479–2482.

20 For further examples of aromatic borylations, see: (*a*) M. J. S. Dewar, V. P. Kubba and R. Pettit, *J. Chem. Soc.*, 1958, 3073–3076; (*b*) X.-Y. Wang, F.-D. Zhuang, R.-B. Wang, X.-C. Wang, X.-Y. Cao, J.-Y. Wang and J. Pei, *J. Am. Chem. Soc.*, 2014, **136**, 3764–3767; (*c*) X.-Y. Wang, F.-D. Zhuang, X.-C. Wang, X.-Y. Cao, J.-Y. Wang and J. Pei, *Chem. Commun.*, 2015, **51**, 4368–4371; (*d*) X.-Y. Wang, D.-C. Yang, F.-D. Zhuang, J.-J. Liu, J.-Y. Wang and J. Pei, *Chem.–Eur. J.*, 2015, **21**, 8867–8873; (*e*) A. John, M. Bolte, H.-W. Lerner and M. Wagner, *Angew. Chem., Int. Ed.*, 2017, **56**, 5588–5592; (*f*) J. S. A. Ishibashi, C. Darrigan, A. Chrostowska, B. Li and S.-Y. Liu, *Dalton Trans.*, 2019, **48**, 2807–2812.

21 For related examples, in which an N-bonded boron electrophile attacks a dangling C═C or C≡C bond rather

than an aryl ring, see: (*a*) H. Wei, Y. Liu, T. Y. Gopalakrishna, H. Phan, X. Huang, L. Bao, J. Guo, J. Zhou, S. Luo, J. Wu and Z. Zeng, *J. Am. Chem. Soc.*, 2017, **139**, 15760–15767; (*b*) A. Abengózar, P. García-García, D. Sucunza, L. M. Frutos, O. Castano, D. Sampedro, A. Pérez-Redondo and J. J. Vaquero, *Org. Lett.*, 2017, **19**, 3458–3461; (*c*) A. Abengózar, D. Sucunza, P. García-García, D. Sampedro, A. Pérez-Redondo and J. J. Vaquero, *J. Org. Chem.*, 2019, **84**, 7113–7122; (*d*) L. Zi, J. Zhang, C. Li, Y. Qu, B. Zhen, X. Liu and L. Zhang, *Org. Lett.*, 2020, **22**, 1499–1503; (*e*) A. Abengózar, I. Valencia, G. G. Otárola, D. Sucunza, P. García-García, A. Pérez-Redondo, F. Mendicuti and J. J. Vaquero, *Chem. Commun.*, 2020, **56**, 3669–3672.

22 A. J. V. Marwitz, E. R. Abbey, J. T. Jenkins, L. N. Zakharov and S.-Y. Liu, *Org. Lett.*, 2007, **9**, 4905–4908.

23 For further examples, see: (*a*) A. J. Ashe and X. Fang, *Org. Lett.*, 2000, **2**, 2089–2091; (*b*) E. R. Abbey, L. N. Zakharov and S.-Y. Liu, *J. Am. Chem. Soc.*, 2010, **132**, 16340–16342; (*c*) A. D. Rohr, J. W. Kampf and A. J. Ashe, *Organometallics*, 2014, **33**, 1318–1321; (*d*) F. Sun, L. Lv, M. Huang, Z. Zhou and X. Fang, *Org. Lett.*, 2014, **16**, 5024–5027; (*e*) A. N. Brown, B. Li and S.-Y. Liu, *J. Am. Chem. Soc.*, 2015, **137**, 8932–8935; (*f*) A. Abengózar, P. García-García, D. Sucunza, A. Pérez-Redondo and J. J. Vaquero, *Chem. Commun.*, 2018, **54**, 2467–2470.

24 J.-S. Lu, S.-B. Ko, N. R. Walters, Y. Kang, F. Sauriol and S. Wang, *Angew. Chem., Int. Ed.*, 2013, **52**, 4544–4548.

25 For further examples, see: (*a*) S. Wang, D. T. Yang, J. Lu, H. Shimogawa, S. Gong, X. Wang, S. K. Mellerup, A. Wakamiya, Y. L. Chang, C. Yang and Z. H. Lu, *Angew. Chem., Int. Ed.*, 2015, **54**, 15074–15078; (*b*) D. T. Yang, S. K. Mellerup, X. Wang, J. S. Lu and S. Wang, *Angew. Chem., Int. Ed.*, 2015, **54**, 5498–5501; (*c*) S. B. Ko, J. S. Lu and S. Wang, *Org. Lett.*, 2014, **16**, 616–619; (*d*) Y. G. Shi, D. T. Yang, S. K. Mellerup, N. Wang, T. Peng and S. Wang, *Org. Lett.*, 2016, **18**, 1626–1629; (*e*) D. T. Yang, Y. Shi, T. Peng and S. Wang, *Organometallics*, 2017, **36**, 2654–2660; (*f*) Y. G. Shi, X. Wang, N. Wang, T. Peng and S. Wang, *Organometallics*, 2017, **36**, 2677–2684; (*g*) W. J. Wu, Q. S. Li and Z. S. Li, *J. Phys. Chem. A*, 2017, **121**, 753–761.

26 M. J. S. Dewar and R. Dietz, *J. Chem. Soc.*, 1960, 1344–1347.

27 W. Maringgele, A. Meller, M. Noltemeyer and G. M. Sheldrick, *Z. Anorg. Allg. Chem.*, 1986, **536**, 24–34.

28 L. M. Greig, B. M. Kariuki, S. Habershon, N. Spencer, R. L. Johnston, K. D. M. Harris and D. Philp, *New J. Chem.*, 2002, **26**, 701–710.

29 Q. J. Zhou, K. Worm and R. E. Dolle, *J. Org. Chem.*, 2004, **69**, 5147–5149.

30 L. M. Greig, A. M. Z. Slawin, M. H. Smith and D. Philp, *Tetrahedron*, 2007, **63**, 2391–2403.

31 M. Numano, N. Nagami, S. Nakatsuka, T. Katayama, K. Nakajima, S. Tatsumi, N. Yasuda and T. Hatakeyama, *Chem.–Eur. J.*, 2016, **22**, 11574–11577.

32 X.-Y. Wang, A. Narita, W. Zhang, X. Feng and K. Müllen, *J. Am. Chem. Soc.*, 2016, **138**, 9021–9024.

33 K. Shigemori, M. Watanabe, J. Kong, K. Mitsudo, A. Wakamiya, H. Mandai and S. Suga, *Org. Lett.*, 2019, **21**, 2171–2175.

34 P. J. Grisdale and J. L. R. Williams, *J. Org. Chem.*, 1969, **34**, 1675–1677.

35 J. He, J. L. Crase, S. H. Wadumethrige, K. Thakur, L. Dai, S. Zou, R. Rathore and C. S. Hartley, *J. Am. Chem. Soc.*, 2010, **132**, 13848–13857.

36 S. Mathew, L. A. Crandall, C. J. Ziegler and C. S. Hartley, *J. Am. Chem. Soc.*, 2014, **136**, 16666–16675.

37 Y. Sumida, R. Harada, T. Kato-Sumida, K. Johmoto, H. Uekusa and T. Hosoya, *Org. Lett.*, 2014, **16**, 6240–6243.

38 A. Budanow, E. von Grotthuss, M. Bolte, M. Wagner and H.-W. Lerner, *Tetrahedron*, 2016, **72**, 1477–1484.

39 T. Katayama, S. Nakatsuka, H. Hirai, N. Yasuda, J. Kumar, T. Kawai and T. Hatakeyama, *J. Am. Chem. Soc.*, 2016, **138**, 5210–5213.

40 H. Saito, K. Nogi and H. Yorimitsu, *Chem. Lett.*, 2017, **46**, 1122–1125.

41 S. Kirschner, S. S. Bao, M. K. Fengel, M. Bolte, H.-W. Lerner and M. Wagner, *Org. Biomol. Chem.*, 2019, **17**, 5060–5065.

42 For corresponding 9,10-thiaboraphenanthrenes, see: F. A. Davis and M. J. S. Dewar, *J. Am. Chem. Soc.*, 1968, **90**, 3511–3515.

43 C. Körner, P. Starkov and T. D. Sheppard, *J. Am. Chem. Soc.*, 2010, **132**, 5968–5969.

44 R. Guo, K.-N. Li, B. Liu, H.-J. Zhu, Y.-M. Fan and L.-Z. Gong, *Chem. Commun.*, 2014, **50**, 5451–5454.

45 L. Benhamou, D. W. Walker, D. K. Bučar, A. E. Aliev and T. D. Sheppard, *Org. Biomol. Chem.*, 2016, **14**, 8039–8043.

46 The Hg(II)-mediated addition of Ph_2BO–H to HC≡COEt has also been reported: M. Murakami and T. Mukaiyama, *Chem. Lett.*, 1982, **11**, 241–244.

47 H. Saito, S. Otsuka, K. Nogi and H. Yorimitsu, *J. Am. Chem. Soc.*, 2016, **138**, 15315–15318.

48 S. Tsuchiya, H. Saito, K. Nogi and H. Yorimitsu, *Org. Lett.*, 2017, **19**, 5557–5560.

49 F. A. Davis and M. J. S. Dewar, *J. Org. Chem.*, 1968, **33**, 3324–3326.

50 F. A. Davis, M. J. S. Dewar and R. Jones, *J. Am. Chem. Soc.*, 1968, **90**, 706–708.

51 B. M. Mikhailov and M. E. Kuimova, *J. Organomet. Chem.*, 1976, **116**, 123–133.

52 J. Chen, Z. Bajko, J. W. Kampf and A. J. Ashe, *Organometallics*, 2007, **26**, 1563–1564.

53 S. Yruegas, D. C. Patterson and C. D. Martin, *Chem. Commun.*, 2016, **52**, 6658–6661.

54 W. Zhang, G. Li, L. Xu, Y. Zhuo, W. Wan, N. Yan and G. He, *Chem. Sci.*, 2018, **9**, 4444–4450.

55 T. Kaehler, M. Bolte, H.-W. Lerner and M. Wagner, *Angew. Chem., Int. Ed.*, 2019, **58**, 11379–11384.

56 S. M. Mathew and C. S. Hartley, *Macromolecules*, 2011, **44**, 8425–8432.

57 Z. Zhou, A. Wakamiya, T. Kushida and S. Yamaguchi, *J. Am. Chem. Soc.*, 2012, **134**, 4529–4532.

58 X. Wang, F. Zhang, J. Gao, Y. Fu, W. Zhao, R. Tang, W. Zhang, X. Zhuang and X. Feng, *J. Org. Chem.*, 2015, **80**, 10127–10133.

59 W. Zhang, F. Zhang, R. Tang, Y. Fu, X. Wang, X. Zhuang, G. He and X. Feng, *Org. Lett.*, 2016, **18**, 3618–3621.

60 C. Zhang, L. Zhang, C. Sun, W. Sun and X. Liu, *Org. Lett.*, 2019, **21**, 3476–3480.

61 S. S. Chissick, M. J. S. Dewar and P. M. Maitlis, *Tetrahedron Lett.*, 1960, **1**, 8–10.

62 G. C. Culling, M. J. S. Dewar and P. A. Marr, *J. Am. Chem. Soc.*, 1964, **86**, 1125–1127.

63 P. J. Comina, D. Philp, B. M. Kariuki and K. D. M. Harris, *Chem. Commun.*, 1999, 2279–2280.

64 P. R. Ashton, K. D. M. Harris, B. M. Kariuki, D. Philp, J. M. A. Robinson and N. Spencer, *J. Chem. Soc., Perkin Trans. 2*, 2001, **11**, 2166–2173.

65 D. J. H. Emslie, W. E. Piers and M. Parvez, *Angew. Chem., Int. Ed.*, 2003, **42**, 1252–1255.

66 M. Lepeltier, O. Lukoyanova, A. Jacobson, S. Jeeva and D. F. Perepichka, *Chem. Commun.*, 2010, **46**, 7007–7009.

67 D. Carnevale, V. del Amo, D. Philp and S. E. Ashbrook, *Tetrahedron*, 2010, **66**, 6238–6250.

68 T. Hatakeyama, S. Hashimoto, S. Seki and M. Nakamura, *J. Am. Chem. Soc.*, 2011, **133**, 18614–18617.

69 X. Wang, F. Zhang, J. Liu, R. Tang, Y. Fu, D. Wu, Q. Xu, X. Zhuang, G. He and X. Feng, *Org. Lett.*, 2013, **15**, 5714–5717.

70 X.-Y. Wang, F.-D. Zhuang, R.-B. Wang, X.-C. Wang, X.-Y. Cao, J.-Y. Wang and J. Pei, *J. Am. Chem. Soc.*, 2014, **136**, 3764–3767.

71 G. Li, W. W. Xiong, P. Y. Gu, J. Cao, J. Zhu, R. Ganguly, Y. Li, A. C. Grimsdale and Q. Zhang, *Org. Lett.*, 2015, **17**, 560–563.

72 A. W. Baggett, F. Guo, B. Li, S.-Y. Liu and F. Jäkle, *Angew. Chem., Int. Ed.*, 2015, **54**, 11191–11195.

73 Z. Lu, H. Quanz, O. Burghaus, J. Hofmann, C. Logemann, S. Beeck, P. R. Schreiner and H. A. Wegner, *J. Am. Chem. Soc.*, 2017, **139**, 18488–18491.

74 S. Nakatsuka, N. Yasuda and T. Hatakeyama, *J. Am. Chem. Soc.*, 2018, **140**, 13562–13565.

75 F. Liu, H. Zhang, J. Dong, Y. Wu and W. Li, *Asian J. Org. Chem.*, 2018, **7**, 465–470.

76 J. Zhang, F. Liu, Z. Sun, C. Li, Q. Zhang, C. Zhang, Z. Liu and X. Liu, *Chem. Commun.*, 2018, **54**, 8178–8181.

77 H. Huang, Y. Zhou, M. Wang, J. Zhang, X. Cao, S. Wang, D. Cao and C. Cui, *Angew. Chem., Int. Ed.*, 2019, **58**, 10132–10137.

78 Y. Appiarius, T. Stauch, E. Lork, P. Rusch, N. C. Bigall and A. Staubitz, *Org. Chem. Front.*, 2021, **8**, 10–17.

79 J. S. A. Ishibashi, J. L. Marshall, A. Mazière, G. J. Lovinger, B. Li, L. N. Zakharov, A. Dargelos, A. Graciaa, A. Chrostowska and S. Y. Liu, *J. Am. Chem. Soc.*, 2014, **136**, 15414–15421.

80 S. Biswas, C. Maichle-Mössmer and H. F. Bettinger, *Chem. Commun.*, 2012, **48**, 4564–4566.

81 M. Müller, C. Maichle-Mössmer and H. F. Bettinger, *Angew. Chem., Int. Ed.*, 2014, **53**, 9380–9383.

82 H. F. Bettinger and M. Müller, *J. Phys. Org. Chem.*, 2015, **28**, 97–103.

83 S. Yruegas, J. J. Martinez and C. D. Martin, *Chem. Commun.*, 2018, **54**, 6808–6811.

84 X. Su, J. J. Baker and C. D. Martin, *Chem. Sci.*, 2020, **11**, 126–131.

85 In a conceptually related fashion, 1,2-dihydro-1,2-azaborines and 1,2-dihydro-1,2-oxaborines have been synthesized through carbene insertion into 1,2-azaborolide and 1,2-oxaborolide anions, respectively: (*a*) A. J. Ashe, X. X. Fang, X. X. Fang and J. W. Kampf, *Organometallics*, 2001, **20**, 5413–5418; (*b*) J. Pan, J. W. Kampf and A. J. Ashe, *Organometallics*, 2004, **23**, 5626–5629. The single or double carbene insertion into 9-borafluorene, which affords six- and seven-membered rings has also been reported: (*c*) T. A. Bartholome, K. R. Bluer and C. D. Martin, *Dalton Trans.*, 2019, **48**, 6319–6322.

86 *Boronic Acids: Preparation and Applications in Organic Synthesis, Medicine and Materials*, ed. D. G. Hall, Wiley-VCH Verlag GmbH & Co. KGaA, Weinheim, Germany, 2nd edn, 2011.

87 L. Hintermann and A. Labonne, *Synthesis*, 2007, **2007**, 1121–1150.

88 W. Liu, H. Wang and C.-J. Li, *Org. Lett.*, 2016, **18**, 2184–2187.

89 We are grateful to one anonymous referee, who brought the following to our attention: in a simplified picture, it can be assumed that there are two particularly important reaction steps in the catalytic cycle: step (1) is the irreversible attack of the B-bonded N/O atom on an η^2-alkynyl–[Au] pre-complex to form vinylic N/O–C═C–[Au] intermediates as resting states (see Scheme 2b). Step (2) is the irreversible proto-demetalation of N/O–C═C–[Au] to give N/O–C═C–H with regeneration of the active catalyst. Step (1) is faster for the BN(Me)–H substrates. Step (2) is faster for the more acidic BO–H substrates and is generally rate-determining. In the cases of independent reactions, this results in a more rapid formation of B,O-PAHs. The situation changes in an intramolecular competition, where most of the catalyst is arrested in the N–C═C–[Au] state, ultimately leading to the B,N-PAH as the main product (here: **8c**). For a related case, see: S. Guo, J. C. Yang and S. L. Buchwald, *J. Am. Chem. Soc.*, 2018, **140**, 15976–15984.

90 J. M. Farrell, C. Mützel, D. Bialas, M. Rudolf, K. Menekse, A.-M. Krause, M. Stolte and F. Würthner, *J. Am. Chem. Soc.*, 2019, **141**, 9096–9104.

91 Z. Liu, J. S. A. Ishibashi, C. Darrigan, A. Dargelos, A. Chrostowska, B. Li, M. Vasiliu, D. A. Dixon and S.-Y. Liu, *J. Am. Chem. Soc.*, 2017, **139**, 6082–6085.

92 M. J. S. Dewar and R. Dietz, *J. Chem. Soc.*, 1959, 2728–2730.

93 M. J. S. Dewar and R. Dietz, *J. Org. Chem.*, 1961, **26**, 3253–3256.

94 M. J. S. Dewar, J. Hashmall and V. P. Kubba, *J. Org. Chem.*, 1964, **29**, 1755–1757.

95 P. Paetzold, C. Stanescu, J. R. Stubenrauch, M. Bienmüller and U. Englert, *Z. Anorg. Allg. Chem.*, 2004, **630**, 2632–2640.

96 J. Pan, J. W. Kampf and A. J. Ashe, *Organometallics*, 2009, **28**, 506–511.
97 G. E. Rudebusch, L. N. Zakharov and S.-Y. Liu, *Angew. Chem., Int. Ed.*, 2013, **52**, 9316–9319.
98 G. A. Molander, S. R. Wisniewski and K. M. Traister, *Org. Lett.*, 2014, **16**, 3692–3695.
99 G. A. Molander, S. R. Wisniewski and J. Amani, *Org. Lett.*, 2014, **16**, 5636–5639.
100 G. A. Molander and S. R. Wisniewski, *J. Org. Chem.*, 2014, **79**, 6663–6678.
101 G. A. Molander, S. R. Wisniewski and E. Etemadi-Davan, *J. Org. Chem.*, 2014, **79**, 11199–11204.
102 F. J. R. Rombouts, F. Tovar, N. Austin, G. Tresadern and A. A. Trabanco, *J. Med. Chem.*, 2015, **58**, 9287–9295.
103 S. Tsuchiya, H. Saito, K. Nogi and H. Yorimitsu, *Org. Lett.*, 2019, **21**, 3855–3860.
104 X. Liu, P. Wu, J. Li and C. Cui, *J. Org. Chem.*, 2015, **80**, 3737–3744.
105 In order to increase the readability of this chapter, we have averaged all NMR chemical shift values of nuclei at the same positions in **4a–6a** on the one hand and **4b–6b** on the other. In the cases of multiplet signals, we have taken the midpoint of each multiplet and averaged those. In all cases the spread of the shift values within the subsets **4a–6a** or **4b–6b** was significantly smaller than the differences in the average values between **4a–6a** and **4b–6b**.
106 H. Nöth and B. Wrackmeyer, *Nuclear Magnetic Resonance Spectroscopy of Boron Compounds, in NMR Basic Principles and Progress*, ed. P. Diehl, E. Fluck and R. Kosfeld, Springer, Berlin, Heidelberg, New York, 1978.
107 M. A. Fox and J. K. Whitesell, *Organic Chemistry*, Jones and Bartlett Publisher, Sudbury, Mass., 3rd edn, 2004.
108 H. L. van de Wouw, J. Y. Lee, M. A. Siegler and R. S. Klausen, *Org. Biomol. Chem.*, 2016, **14**, 3256–3263.
109 The corresponding methylamino borane did not undergo the cyclization reaction to furnish a parent $(B,N)_2$-perylene devoid of C-bonded substituents.
110 T. Ishiyama, J. Takagi, J. F. Hartwig and N. Miyaura, *Angew. Chem., Int. Ed.*, 2002, **41**, 3056–3058.
111 T. Ishiyama, Y. Nobuta, J. F. Hartwig and N. Miyaura, *Chem. Commun.*, 2003, 2924–2925.
112 I. A. I. Mkhalid, J. H. Barnard, T. B. Marder, J. M. Murphy and J. F. Hartwig, *Chem. Rev.*, 2010, **110**, 890–931.
113 H. Tamura, H. Yamazaki, H. Sato and S. Sakaki, *J. Am. Chem. Soc.*, 2003, **125**, 16114–16126.
114 D. N. Coventry, A. S. Batsanov, A. E. Goeta, J. A. K. Howard, T. B. Marder and R. N. Perutz, *Chem. Commun.*, 2005, 2172–2174.
115 For B-monosubstituted 2,1-B,N-benzenes and suitable 2,1-B,N-naphthalenes, Liu *et al.* and Molander *et al.* have shown that the Ir-catalyzed C–H borylation occurs preferentially at the most acidic hydrogen atoms and therefore as close as sterically possible to the embedded electronegative N atoms: (*a*) G. H. M. Davies, M. Jouffroy, F. Sherafat, B. Saeednia, C. Howshall and G. A. Molander, *J. Org. Chem.*, 2017, **82**, 8072–8084; (*b*) A. W. Baggett, M. Vasiliu, B. Li, D. A. Dixon and S.-Y. Liu, *J. Am. Chem. Soc.*, 2015, **137**, 5536–5541; (*c*) A. W. Baggett, F. Guo, B. Li, S.-Y. Liu and F. Jäkle, *Angew. Chem., Int. Ed.*, 2015, **54**, 11191–11195; (*d*) C. R. McConnell, F. Haeffner, A. W. Baggett and S. Y. Liu, *J. Am. Chem. Soc.*, 2019, **141**, 9072–9078. Based on an investigation of various quinoline and nonsymmetrical 1,2-disubstituted benzene substrates, Marder, Steel *et al.* have found that preferential borylation occurs at the site of the most deshielded H/C atom in the $^{1}H/^{13}C\{^{1}H\}$ NMR spectrum (provided that it is sterically accessible): (*e*) H. Tajuddin, P. Harrisson, B. Bitterlich, J. C. Collings, N. Sim, A. S. Batsanov, M. S. Cheung, S. Kawamorita, A. C. Maxwell, L. Shukla, J. Morris, Z. Lin, T. B. Marder and P. G. Steel, *Chem. Sci.*, 2012, **3**, 3505–3515.In the case of **9** (and also of pristine 2,1-B,N-benzene), the ^{1}H-NMR tool failed to provide a correct prediction, whereas the ^{13}C-NMR tool worked faithfully (*cf.* the NMR data given in the ESI†).
116 J. Merz, A. Steffen, J. Nitsch, J. Fink, C. B. Schürger, A. Friedrich, I. Krummenacher, H. Braunschweig, M. Moos, D. Mims, C. Lambert and T. B. Marder, *Chem. Sci.*, 2019, **10**, 7516–7534.
117 J. Merz, L. Dietrich, J. Nitsch, I. Krummenacher, H. Braunschweig, M. Moos, D. Mims, C. Lambert and T. B. Marder, *Chem.–Eur. J.*, 2020, **26**, 12050–12059.
118 Shinokubo *et al.* succeeded in the Ir-catalyzed direct tetraborylation of perylene bisimides, which took place at the same sites as in the case of **9** despite the presence of *ortho*-substituents: T. Teraoka, S. Hiroto and H. Shinokubo, *Org. Lett.*, 2011, **13**, 2532–2535.